Geophys. Astrophys. Fluid Dynamics, 1982, Vol. 19, pp. 311–330
0309-1929/82/1904-0311 $06.50/0

High-Speed Streams from Coronal Holes and the Accelerating Mechanism of the Solar Wind

WEN-RUI HU
Institute of Mechanics, Academia Sinica, Beijing, China

(*Received April 3, 1981*)

In this paper, the general Mach number equation is derived, and the influence of typical energy forms in the solar wind is analysed in detail. It shows that the accelerating process of the solar wind is influenced critically by the form of heating in the corona, and that the transonic mechanism is mainly the result of the adjustment of the variation of the cross-section of flowing tubes and the heat source term.

The accelerating mechanism for both the high-speed stream from the coronal hole and the normal solar wind is similar. But, the temperature is low in the lower level of the coronal hole and more heat energy supply in the outside is required, hence the high speed of the solar wind; while the case with the ordinary coronal region is just the opposite, and the velocity of the solar wind is therefore lower. The accelerating process for various typical parameters is calculated, and it is found that the high-speed stream may reach 800 km/sec.

1. INTRODUCTION

According to the theory of the solar wind developed by Parker (1958, 1965), if a constant temperature atmosphere is maintained near the sun, it will produce an expanding flow of the corona gas. This led to discussions of the problem of the energy source in the solar wind (see, Scarf, 1966; Barnes, 1974). After the discovery of the association of the coronal hole with the high-speed stream of the solar wind, the problem of the energy source became more prominent. The problem of the energy source is a key problem, because we have to find out what type of energy source can drive the solar wind and accelerate its flow.

The energy flux in the solar wind is closely related to the heating of the corona. As the density of plasma in the corona decreases rapidly, the quantity of energy required to heat the corona is only about 0.01 of the quantity of wave energy transported from the convective region. The propagating and dissipating processes of the transporting wave energy are closely related to the heating of the corona, and therefore closely related to the heat source in the solar wind. Such energy sources are confined by the magnetic field at the solar atmosphere. The configuration in the open coronal field facilitates the supply of large quantities of transporting wave energy into the solar wind, thus producing high-speed streams.

In the theory of the solar wind, it is usually through the polytropic assumption that the influence of the energy source term is included. When the problem is dealt with in such a simplified manner, the transonic mechanism is the result of the mutual adjustment of the changing effect of the expanding cross-section and the influence of gravity. It seems that there is an influence on the transonic mechanism if the heat energy source term is included in the parameters of the process, and the accelerating mechanism is obviously influenced by the heating process.

Holzer (1977) discussed in general the influence of the addition of heat and momentum on the solar wind and stellar wind. Recently, Leer and Holzer (1980) analyzed the addition of energy in the solar wind in detail. In this paper, the discussion is concentrated on the influence of the heat flux on the accelerating process of the solar wind, and the ideas are applied to explain the high-speed stream from the coronal hole. The approach of this paper is similar to the one of Holzer (1977).

The equations for the one-dimensional flow of the solar wind are:

$$\frac{d}{dr}(\rho v A)=\frac{dm}{dr}, \tag{1.1}$$

$$v\frac{dv}{dr}=-\frac{1}{\rho}\frac{dp}{dr}+\frac{d\psi}{dr}, \tag{1.2}$$

$$\frac{de}{dt}+p\frac{d}{dr}\left(\frac{1}{\rho}\right)=\frac{dq}{dr}, \tag{1.3}$$

$$p=\rho\mathscr{R}T, \tag{1.4}$$

where p, ρ, T, v, e represent gaseous pressure, density, temperature, velocity and internal energy respectively. Also, $m(r)$ denotes the mass flux, $\mathscr{R}$ the gas constant, and $q(r)$ is the heat due to both the heat source q_1 added from the outside of the flowing tube and the heat q_2 dissipated by wave energy, that is $dq/dr=dq_1/dr+A^{-1}\,d(Aq_2)/dr$.

For simplicity, we shall consider $q(r)$ as the total heat source. The potential ψ includes the gravitational potential $GM_\odot/r$ and the potential of other forces. The sonic velocity here is

$$a^2=(\partial p/\partial \rho)_s=\gamma \mathscr{R} T, \tag{1.5}$$

where γ is the ratio of the specific heats. For a monoatomic gas, $\gamma=5/3$. By using the Eqs. (1.2) and (1.3), we can derive the relation for the enthalpy $i=e+p/\rho$ as follows:

$$\frac{di}{dr}+\frac{d}{dr}(\tfrac{1}{2}v^2)-\frac{d\psi}{dr}=\frac{dq}{dr}. \tag{1.6}$$

From this we find, by integration, the relation for the energy source:

$$i+\tfrac{1}{2}v^2-\psi-q=E, \tag{1.7}$$

where the constant of integration, E, is the total energy. By using (1.5), Eq. (1.7) can be rewritten as follows:

$$a^2/(\gamma-1)+\tfrac{1}{2}v^2-\psi-q=E. \tag{1.8}$$

Far from the sun, $\psi\to 0$, $q\to q_\infty$; and it may be determined:

$$E=a_\infty^2/(\gamma-1)+\tfrac{1}{2}v_\infty^2-q_\infty. \tag{1.9}$$

The energy E is determined by v_∞^2 and q_∞. On the other hand, there is also:

$$E=a_0^2/(\gamma-1)+\tfrac{1}{2}v_0^2-\psi_0-q_0. \tag{1.10}$$

The subscript 0 corresponds to the initial value at the lower level of the corona. As the values of v_0 and a_∞ are small, the energy added to the solar wind can be given by using (1.9) and (1.10) as follows:

$$q_\infty-q_0=(a_\infty^2-a_0^2)/(\gamma-1)+\tfrac{1}{2}(v_\infty^2-v_0^2)+\psi_0 \tag{1.11}$$

$$=-a_0^2/(\gamma-1)+\tfrac{1}{2}v_\infty^2+\psi_0. \tag{1.12}$$

The Eq. (1.12) shows that, in order to overcome the gravitational field ψ_0 near the solar surface and to accelerate a particle to the velocity v_∞, an energy $q_\infty - q_0$ must be supplied to the solar wind in addition to the initial heat energy $a_0^2/(\gamma-1)$. The gravitational potential at the solar surface is very strong:

$$\psi_0|_{r=1.1r_\odot} = GM_\odot/(1.1r_\odot) \approx 1.7334 \times 10^{15}\ \mathrm{cm^2/sec^2}. \tag{1.13}$$

The velocity of the solar wind near the earth's orbit is 400–800 km/sec. If we take the temperature of the corona as 2×10^6 K, then

$$\tfrac{1}{2}v_\infty^2|_{r=1\,\mathrm{AU}} \approx (0.8-3.2) \times 10^{15}\ \mathrm{cm^2/sec^2}, \tag{1.14}$$

$$[a_0^2/(\gamma-1)]|_{T_0=2\times10^6\mathrm{K}} \approx 0.831 \times 10^{15}\ \mathrm{cm^2/sec^2}. \tag{1.15}$$

Hence, an energy density of about $1.7 \times 10^{15}\ \mathrm{cm^2/sec^2}$ must be applied to the normal solar wind, and $4.1 \times 10^{15}\ \mathrm{cm^2/sec^2}$ to the high-speed stream from the coronal hole. On the surface of the sun, the gravitational potential is fundamental, the variation of a_0 is not considerable, and the velocity of the solar wind on the amount of the energy added. No solar wind could be produced without the addition of sufficient energy.

In this paper there is a general discussion on the accelerating mechanism of the solar wind. The influence of various forms of energy distribution on the accelerating process of the solar wind is analysed, and the quantitative characteristics of the normal solar wind and the high-speed stream from the coronal hole are derived.

2. THE EQUATIONS OF THE SOLAR WIND AND THE QUALITATIVE CHARACTERISTICS OF THEIR SOLUTIONS

The basic equations describing the solar wind are (1.1)–(1.4). From the state Eq. (1.4), we obtain:

$$\frac{dp}{dr} = \mathscr{R}\left(T\frac{d\rho}{dr} + \rho\frac{dT}{dr}\right).$$

By using the relation of energy conservation, the above formula may be converted as follows:

$$\frac{dp}{dr} = \frac{a^2}{\gamma}\frac{d\rho}{dr} + \frac{\gamma-1}{\gamma}\rho\left[\frac{dq}{dr} + \frac{d\psi}{dr} - \frac{d}{dr}(\tfrac{1}{2}v^2)\right]. \tag{2.1}$$

Substituting (2.1) into the momentum equation and using (1.1), we obtain

$$\frac{v^2-a^2}{v}\frac{dv}{dr}=\frac{a^2}{A}\frac{dA}{dr}-\frac{a^2}{m}\frac{dm}{dr}-\frac{GM_\odot}{r^2}+f_*-(\gamma-1)\frac{dq}{dr}, \tag{2.2}$$

where f_* represents the external forces other than gravity. This equation gives the influence of different effects on the flow field. For subsonic flow, the accelerating factor of the solar wind is given as $dA/dr<0$, $dm/dr>0$, $-GM_\odot/r^2+f_*<0$, $dq/dr>0$: and for supersonic flow, the case is just the opposite.

The sonic velocity a is a function of temperature. Equation (2.2) can be integrated directly in the case of constant temperature. In normal cases, a is related to v. Let us use (1.8), and convert (2.2) into an equation for the Mach number:

$$\left(\frac{M^2-1}{2M^2}\right)\frac{dM^2}{dr}=[1+\tfrac{1}{2}(\gamma-1)M^2]\left[\frac{1}{A}\frac{dA}{dr}-\frac{1}{m}\frac{dm}{dr}\right.$$
$$\left.+\frac{1}{2}\left(\frac{\gamma+1}{\gamma-1}\right)(E+\psi+q)^{-1}\frac{d\psi}{dr}-\tfrac{1}{2}(\gamma M^2+1)(E+\psi+q)^{-1}\frac{dq}{dr}\right], \tag{2.3}$$

where $M=v/a$. Equation (2.3) contains only M and some given functions of r, and describes completely the mechanism of the accelerating process of the solar wind.

Now, we shall discuss specifically the cases in which the flux in the flow direction remains unchanged (m=constant), the external force is absent except for gravity ($f_*=0$), and we shall assume that the variation of the cross-section of the flow tube is given by $A=A_0r^s$. We introduce the non-dimensional parameters:

$$R=\frac{r}{r_\odot},\quad E_0=\frac{E}{GM_\odot/r_\odot},\quad Q_0=\frac{q_0}{GM_\odot/r_\odot}. \tag{2.4}$$

The non-dimensional heat source is expressed as:

$$\frac{q}{GM_\odot/r_\odot}=Q_0f(R). \tag{2.5}$$

In order to show clearly the influence of gravity, the non-dimensional gravitational potential term may be expressed as

$$G_0 = \frac{\psi_0}{GM_\odot/r_\odot} = 1.$$

From (2.3), we obtain:

$$\frac{dM^2}{dR} = \frac{2M^2[1+\frac{1}{2}(\gamma-1)M^2]}{M^2-1}\left[\frac{E_0 S}{R} + \frac{(2S-1)\gamma-(2S+1)}{2(\gamma-1)}\cdot\frac{G_0}{R^2}\right.$$

$$\left. + Q_0 S\frac{f(R)}{R} - \tfrac{1}{2}(\gamma M^2+1)Q_0 f'(R)\right]\left[E_0 + \frac{G_0}{R} + Q_0 f(R)\right]^{-1}. \qquad (2.6)$$

The most general case is that of spherical expansion, $s=2$; and $\gamma=5/3$ for a monoatomic gas. Then, the coefficient of the gravitational term in the numerator of Eq. (2.6) is zero, that is $(2S-1)\gamma-(2S+1)=0$. Equation (2.6) may then be simplified as:

$$\frac{dM^2}{dR} = \frac{4}{R}\left[\frac{M^2(1+M^2/3)Q_0}{E_0+G_0/R+Q_0 f(R)}\right]\left[\frac{-(1/4)(1+5M^2/3)Rf'(R)+f(R)+E_0/Q_0}{M^2-1}\right]. \qquad (2.7)$$

The above formula shows that at the sonic singularity point $M=1$, $R=R_*$ must satisfy the relation:

$$-2R_* f'(R_*)/3 = -E_0/Q_0 - f(R_*), \qquad (2.8)$$

where R_* is the position of the sonic points. Consequently, the accelerating process and the transonic mechanism are mainly determined by both the variation of the cross-section of the flow and the form of the heat source. According to the usual theories of the solar wind, the accelerating process is mainly conditioned by the adjustment of the gravitation and the variation of the cross-section, and is the result of the simplification of the energy form. But, in fact, the distribution of the energy source in the corona must have considerable influence on the accelerating process of the solar wind. It requires further research to explain why the gravitational term disappears from the numerator of Eq. (2.6) when $\gamma=(2S-1)/(2S+1)$. It is necessary to consider the influence of gravitational effects on the singular property of the solar wind Eq. (2.6) if $\gamma \neq (2S-1)/(2S+1)$.

The accelerating process near the surface of the sun is determined by the properties of the sonic singular point $M=1$, $R=R_*$. For the sake of convenience, Eq. (2.7) may be written as:

$$dM^2/dR=\beta(M^2,R)P(R,M^2)/(M^2-1) \tag{2.9}$$

where $\beta(M^2,R)$ is the regular term, and $P(R,M^2)$ the singular numerator, that is:

$$\beta(M^2,R)=\frac{4}{R}\frac{(1+M^2/3)Q_0}{Q_0f(R)+1/R+E_0}>0, \tag{2.10}$$

$$P(R,M^2)=-\tfrac{1}{4}(1+5M^2/3)Rf'(R)+f(R)+E_0/Q_0. \tag{2.11}$$

The singular properties of Eq. (2.9) are determined by those of the following equation:

$$dM^2/dR=\beta_0[P'_R(R_*,1)(R-R_*)-P'_{M^2}(R_*,1)(M^2-1)]/(M^2-1), \tag{2.12}$$

where $\beta_0=\beta(1,R_*)$. From the characteristic equation of (2.12)

$$\begin{vmatrix}\lambda-\beta_0P'_{M^2}(R_*,1) & -P'_R(R_*,1)\\ -1 & \lambda\end{vmatrix}=0,$$

it is possible to find the two characteristic roots, namely

$$\lambda_{1,2}=\tfrac{1}{2}\{\beta_0P'_{M^2}(R_*,1)\pm[\beta_0^2P'^2_{M^2}(R_*,1)+4P'_R(R_*,1)]^{1/2}\}, \tag{2.13}$$

How the value of the characteristic roots decides the properties of the singular points may be summarized as follows:

1) If we satisfy the condition

$$P'_R(R_*,1)=\tfrac{1}{3}f'(R_*)-\tfrac{2}{3}R_*f''(R_*)>0, \tag{2.14}$$

then λ_1,λ_2 are a pair of real roots with opposite signs, and the sonic point is a saddle point.

2) If we satisfy the condition

$$0<4P'_R(R_*,1)+\beta_0^2P'^2_{M^2}(R_*,1)<\beta_0^2P'^2_{M^2}(R_*,1), \tag{2.15}$$

then λ_1, λ_2 are real roots with the same sign and the sonic singular point is a nodal point.

3) If we satisfy the condition

$$4P'(R_*, 1) + \beta_0^2 P'^2_{M^2}(R_*, 1) < 0, \tag{2.16}$$

then λ_1, λ_2 are a pair of complex conjugate roots. When $P'_{M^2}(R_*, 1) = 0$, the sonic point is the singular point of centre type; and when $P'_{M^2}(R_*, 1) \neq 0$, the singularity is at the focal point.

Hence it is possible to describe qualitatively the flow properties of the solar wind in the corona according to the form of the distribution of the source $f(R)$. As there may be more than one sonic singular point, the flow property will be determined by the whole configuration of integrated curves which is given by whole singular points.

As there is energy flow continually added to the solar wind, the general trend of $f(R)$ increases with R. Without losing the generality, let us take

$$f(0) = 0, \qquad f(\infty) = 1. \tag{2.17}$$

The most general distribution for $f(R)$ increases gradually from zero to 1, shown as curves I and II in Figure 1. It can be shown that $f''(R) < 0$ for curve I. For curve II, there is a turning point at $R = R_t$, since $f''(R) > 0$ if $R < R_t$, and $f''(R) < 0$ when $R > R_t$. Another type of energy source fluctuates with the height, and heat is added and removed accordingly along the flow direction, as shown in curve III.

The energy distribution of type I satisfies condition (2.14), and there is only one sonic point which is a saddle point. The configuration of the integrated curve is shown in Figure 2. This is similar to the property of the singular point in the general theory of the solar wind, but it is determined by both the cross-section effect and heat source effect.

As to the heat source distribution of curve II, if the position of the singular point is beyond the turning point, i.e. $R_* > R_t$, then the singular point will be a saddle point, and the integrated curve is similar to that in Figure 2; if $R_* < R_t$ and the variation of its inclination is not considerable, then the singular point will still be a saddle one; otherwise it will be either a node or a focal point. There cannot exist a smooth transonic flow in the one-dimensional flow if there is only one singular point which is not a saddle one. If there are two singular points at the same time, then the one in the region $R_* > R_t$ must be a saddle point. In such a case, there still exists the transonic flow, and the configuration of the integrated curve is shown in Figure 3.

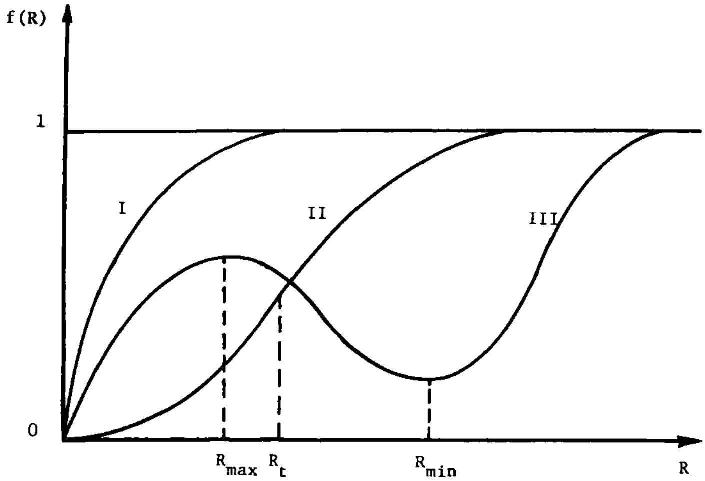

FIGURE 1 The typical curve of a heat source distribution.

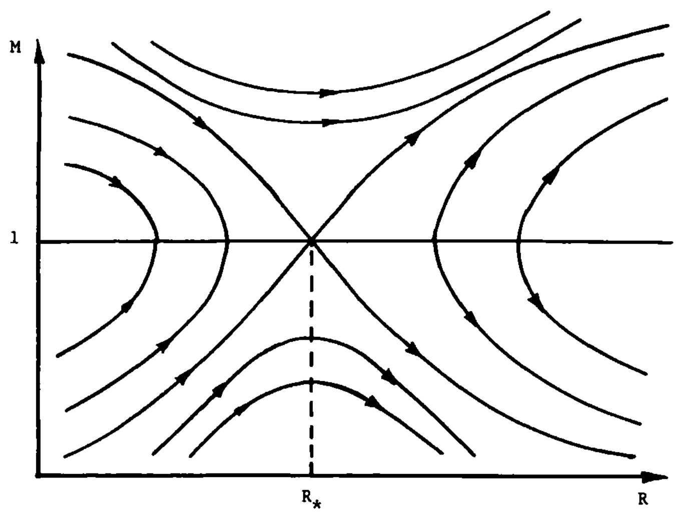

FIGURE 2 The integrated curves corresponding to condition (2.14).

The curve III in Figure 1 is a typical wave distribution. The energy is supplied to the flow in the regions $R<R_{max}$ and $R>R_{*2}$, hence $f'(R)>0$ and $f''(R)<0$, so the singular points must be saddle points. In the region $R_{max}<R<R_{min}$, we have $f'(R)<0$, and $f''(R)$ will turn from negative to positive, so the singular points are mainly nodal ones or focal ones. The

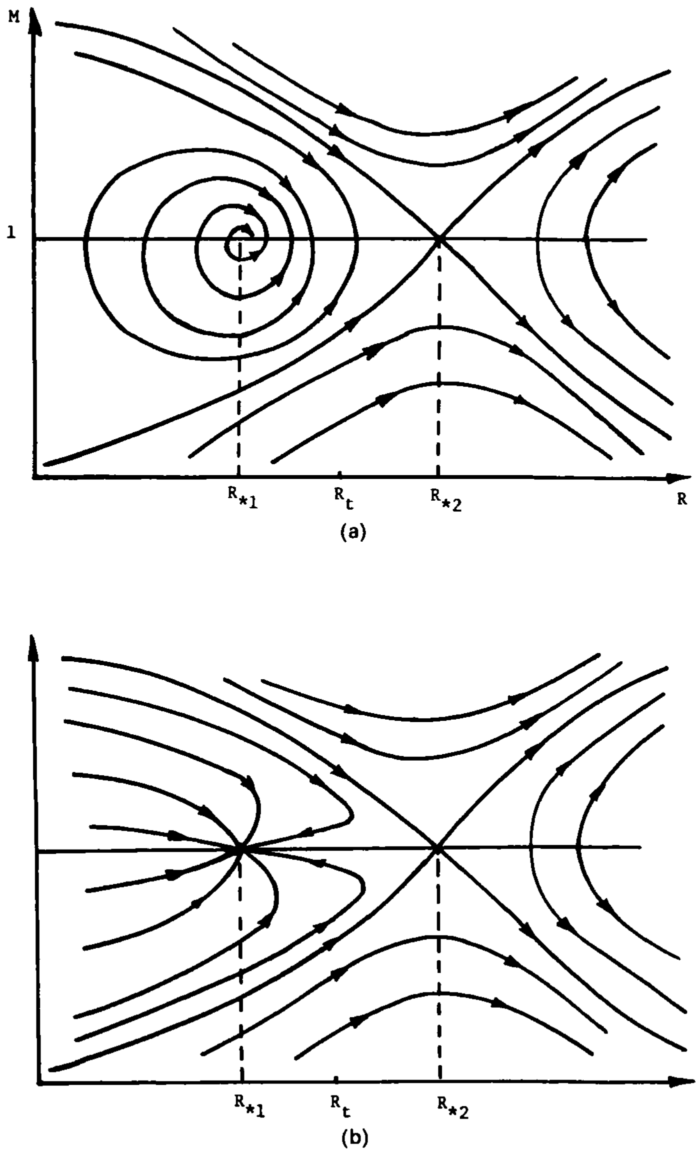

FIGURE 3 The integrated curves corresponding to curve II in Figure 1 when there exist two singular points.

(*a*) Combination of saddle point and focal point.

(*b*) Combination of saddle point and nodal point.

type of the singular points in $R_{min} < R < R_*$ is similar to that shown for curve II. If there are two singular points at the same time, the integrated curve is similar to Figure 3, but the position of the saddle point may be inside the focal or nodal point. If these are three singular points at the same time, some possible configurations are shown in Figure 4.

The properties of the solar wind flow field in the local one-dimensional flow depend mainly on the distribution of the heat source, or on the number and type of the singular points in Eq. (2.7). The number of singular points is determined by the roots of Eq. (2.8). As $-1 < E_0 < 0$ and $0 \leqq f(R) \leqq 1$, then $|E_0|/Q_0 - f(R)$ on the right-hand side of (2.8) turns from positive to negative, and approaches $-(1 - |E_0|/Q_0)$ when R is comparatively large. Thus, when R is large, $Rf'(R)$ must be small. Therefore, at least in the region of large R, there may be a singular point at $R = R_*$, which satisfies (2.8). When R is large, all the curves in Figure 1 satisfy the conditions $f'(R_*) > 0$ and $f''(R_*) < 0$, and the singular point will be a saddle one. If at least one of the singular points is a saddle point, then there generally exists a smooth transonic flow. The general trend is to add energy to the solar wind in the corona, so that supersonic solar flow could be obtained in most one-dimensional flow tubes. Even if there is no supersonic flow in a few flow tubes, the final average property of the solar wind is supersonic because of the interaction of the flow.

The configurations of the integrated curves given here are similar to the ones in figures 2 and 3 of Holzer (1977). However, in this paper, we point out that the number of singular points depends on the distribution of energy addition in the solar wind. There may be only one or two sonic points if the function $f(R)$ is increased monotonically, and this seems to be the most common case. Furthermore, the aligned directions of the integrated curves are pointed out, so the configurations are reasonable. In the case of three singular sonic points with two saddle ones and one focal one, the configuration in Figure 4a is also different from the configuration given by Holzer (1977).

3. QUANTITATIVE FEATURES OF THE SOLAR WIND AND THE HIGH STREAM FROM THE CORONAL HOLE

The heating of the solar atmosphere is one of the important problems in solar physics. It is generally believed that the sonic wave, emitted by the turbulence in the solar convective region, is either propagated into the solar atmosphere and dissipated, or developed into shock waves and dissipated, heating the chromosphere. The observations show that the

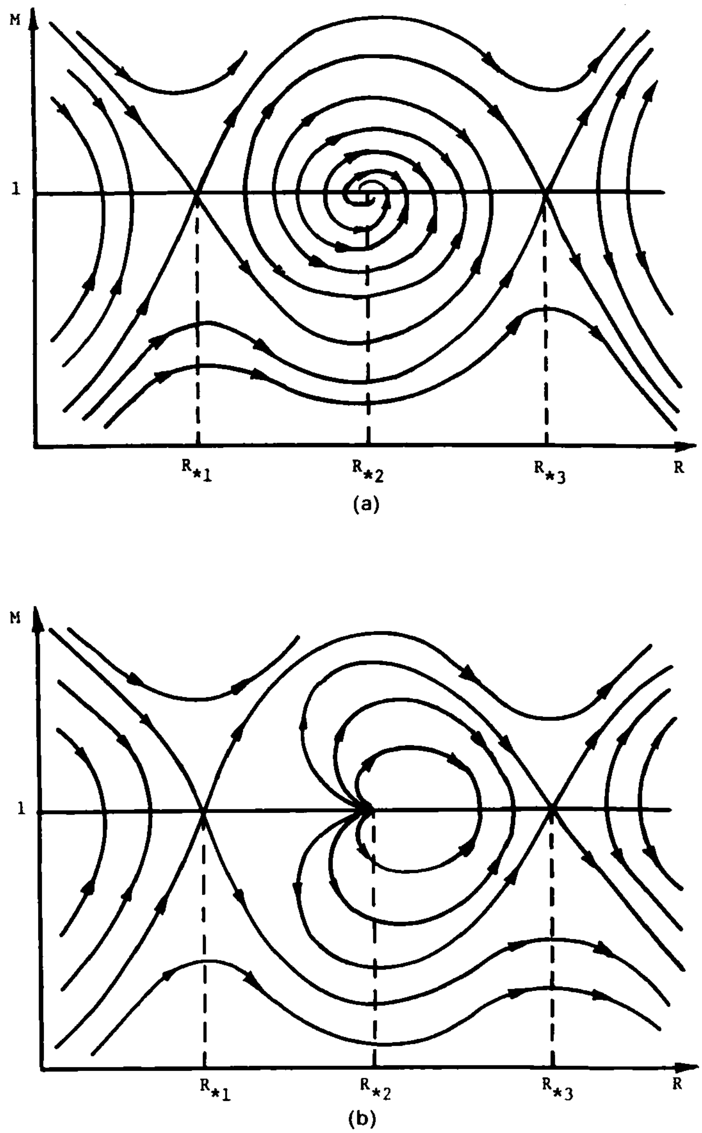

FIGURE 4 The integrated curves corresponding to curve III in Figure 1 when there exist three singular points.

(*a*) Combination of two saddle points and a focal point.

(*b*) Combination of two saddle points and a nodal point.

magnetohydrodynamic waves can propagate into the corona (Cheng *et al.*, 1979). If there is a strong magnetic field in the convective region, the energy flux of the MHD wave could be larger than an order of magnitude of the sonic one, which is about 10^7 erg/cm^2 sec (Osterbrock, 1963). If the coronal velocity is taken as 50 km/sec, then the wave energy flux will be

$$q=\pi F_+/(\rho v)\approx 1.7\times(10^{17}-10^{18})\,\mathrm{erg/g},$$

which is two or three orders of magnitude larger than the gravitational potential energy (1.13) at the solar surface. In principle, the supply of a heat source for the acceleration of the solar wind is out of the question.

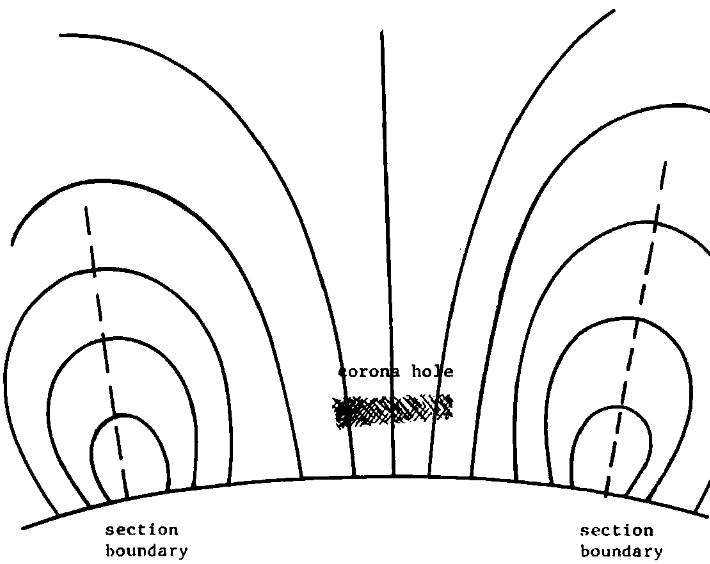

FIGURE 5 Configuration of the magnetic field corresponding to the coronal hole.

Specifically, the coronal hole is located between two regions of the large-scale closed magnetic field. The magnetic field in the coronal hole is open as shown in Figure 5. The wave energy flux excited in the active region is originally larger, and the magnetic field above it is closed, so the energy of the MHD wave is dissipated in large amounts at the top of the magnetic field arc. This makes the temperature at the lower corona even higher and the heat at the outside less intense in the active region. The situation is just the opposite in the coronal hole. Besides, when the Alfvén wave in the closed magnetic field is propagated along the magnetic arc, it could be converted into an MHD wave (Wenzel, 1974), a part of such a wave being propagated into the region of open magnetic field above the coronal hole. In addition to this, as a result of the refractive effect, the magnetosonic wave in the strong field region can be propagated into the weak field region (Hu, 1980). It will be seen from this that the temperature at the coronal hole corresponding to the lower corona is comparatively low, but the heat flux outside is large; while the temperature for the ordinary solar wind corresponding to the lower level corona is comparatively high, but the heat flux outside is small. As the acceleration of the solar wind is mainly decided by the heat source, the corresponding region of the corona is the high velocity stream.

The local accelerating process can be speeded up if the expanding cross-section of the open magnetic field tube diverges rapidly (Kopp and Holzer, 1976; Rosner and Vaiana, 1977; Whang and Chien, 1978). As the temperature effect at the distant regions is very weak, the total accelerating process is mainly determined by the heat source. Whether the cross-section of the flow tube can be changed rapidly or not is also an assumption that requires further study.

The flow parameters of the solar wind can be calculated if the distribution function of the energy source $f(R)$ is given. For the sake of convenience, let us concentrate on the distribution function shown in curve I of Figure 1. We may take:

$$f(R)=1-\exp[(-R+R_0)/R_1], \tag{3.1}$$

where R_0 is the initial position, and R_1 is the typical decay length for the supplying heat. It is not difficult to prove that the derivative of $f(R)$ in (3.1) satisfies the condition (2.14), because

$$f'(R)=R_1^{-1}\exp[-(R-R_0)/R_1]>0$$

$$f''(R)=R_1^{-2}\exp[-(R-R_0/R_1]<0. \tag{3.2}$$

Therefore, the sonic singular point is a saddle point. Substituting (3.1) into (2.8), the right-hand side of (2.8) becomes a monotonically increasing function, while the left-hand side of (2.8) has a maximum value at $R=R_1$, and is monotonic on either side of $R=R_1$. Generally, there is only one singular point for such a distribution of the heat source, and its qualitative characteristic is shown in Figure 2.

Substituting (3.1) into (2.6), we can solve the initial value problem of

Eq. (2.7) by quantitative calculation for the given initial value:

$$M=M_0, \quad \text{when} \quad R=R_0. \tag{3.3}$$

The sonic point is a singular point, which is very sensitive to the variation of the initial value. Given any initial value (3.3), it does not correspond exactly to the solution of the smooth transonic flow. A better method is to start the calculation from the sonic point $M=1$, $R=R_*$. Using (2.6) to find the limit as $M\to 1$ or $R\to R_*$ of M^2, we shall obtain:

$$\left(\frac{dM^2}{dR}\right)^2_{R=R_*}+\frac{\alpha\gamma}{2S}R_*f'(R_*)\left(\frac{dM^2}{dR}\right)_{R=R_*}$$
$$+\alpha\left[\frac{\gamma+1}{2S}R_*f''(R_*)+\frac{\gamma+1-2S}{2S}f'(R_*)\right]=0 \tag{3.4}$$

where the coefficient α is given by

$$\alpha=[(\gamma+1)SQ_0]/\{R_*[E_0+Q_0f(R_*)+R_*^{-1}]\}. \tag{3.5}$$

From (3.4), it is possible to determine the derivative at the singular point:

$$\left(\frac{dM^2}{dR}\right)_{R=R_*}=\frac{1}{2}\left\{-\frac{\alpha\gamma}{2S}R_*f'(R_*)\pm\left[\frac{\alpha^2\gamma^2}{4S^2}[R_*f'(R_*)]^2\right.\right.$$
$$\left.\left.+4\alpha\left[-\frac{\gamma+1}{2S}R_*f'(R_*)+\frac{2S-1-\gamma}{2S}f'(R_*)\right]\right]^{1/2}\right\}. \tag{3.6}$$

Using Eq. (3.1), and taking $s=2$, $\gamma=5/3$, we obtain:

$$\left(\frac{dM^2}{dR}\right)_{R=R_*}=-\frac{5\alpha}{24}\left(\frac{R_*}{R_1}\right)e^{-R_*/R_1}\pm\left[\frac{25\alpha^2}{576}\left(\frac{R_*}{R_1}\right)^2e^{-2R_*/R_1}\right.$$
$$\left.+\frac{\alpha}{3R_1}\left(1+\frac{2R_*}{R_1}\right)e^{-R_*/R_1}\right]^{1/2}. \tag{3.7}$$

The above formula shows that there are two real characteristic directions at the sonic point which must be a saddle point. If the positive sign before the square root is taken, it corresponds to the solar wind accelerating from subsonic to supersonic flow. The Mach number $1\pm\Delta M$ at $R_*\pm\Delta R$

can be obtained by using Eq. (3.7), and then the solution with transonic flow can be obtained.

According to the values of the temperature and velocity at the solar surface $R = R_0$, the value of E_0 can be given by using (2.10). We have calculated the following three cases:

$$E_0 = -0.8755, \quad -0.7557, \quad -0.5160,$$

which correspond to temperatures at the lower corona of 5×10^5, 1×10^6, 2×10^6 K respectively. The case of the lowest temperature at the lower corona corresponds to the high-speed stream of the coronal hole, and the case of the high temperature corresponds to that of the ordinary flow of the solar wind. In the case when a heat of Q_0 is supplied, we shall be able to calculate the flow parameters of the solar wind, the value of Q_0 in the calculation varying from 2.7 to 0.7. According to Eq. (1.12), a large value for Q_0 corresponds to a high-speed stream, and a small value for Q_0 corresponds to a low-speed stream.

Figure 6 illustrates the several types of velocity distribution. If enough energy is supplied (i.e., if Q_0 is large enough), then the velocity of the solar wind can reach high speeds, e.g., 700–800 km/sec. In Figure 6, the distribution of velocity corresponding to the four different values of Q_0 with $E_0 = -0.7557$ is given. This shows clearly that the larger the Q_0, the larger the velocity. Hence, the flow from the coronal hole corresponds to the high-speed stream.

Several typical temperature profiles are given in Figure 7. If the heat flux is large, there will be a peak temperature at the outer corona, but there will not be much variation in the coronal temperature; it is nearly the case of constant temperature at the solar surface ana then it expands. Parker's theory assumes that the constant temperature extends to 20 solar radii and this implies that a large amount of energy flux should be supplied. Figure 7 also gives the temperature profiles for the same parameters, but with different R_1. It may be expected that, the larger the extension of the region of heat supply, i.e., the larger R_1 gets, the higher the temperature becomes. In Figure 7, the peak temperature may be a little higher in the case of larger Q_0, and it will be better if the heat conductivity is considered.

Figure 8 shows the profiles of relative densities in the solar atmosphere. The results of calculation show that for similar values of E_0 and R_1, the density profiles for different values of Q_0 are almost the same. As R_1 increases, the gradients will also increase. The dotted lines in Figure 8 are the observed results. The trend of the results of both observation and calculation agree.

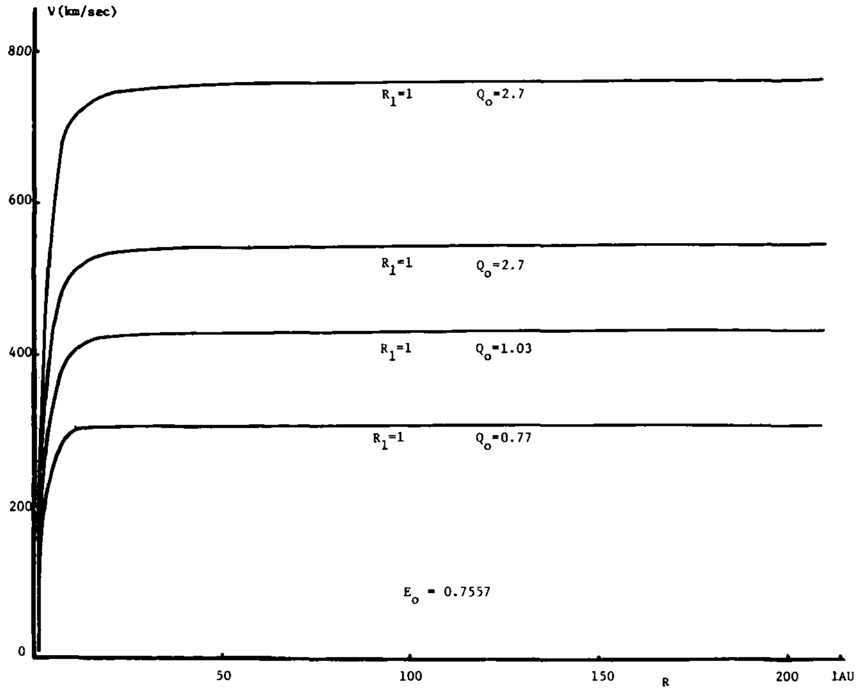

FIGURE 6 Several typical velocity distributions of the solar wind.

TABLE I
Critical radius R_* for $E_0 = -0.8755$.

	$Q_0=2.7$	$Q_0=2.0$	$Q_0=1.6$	$Q_0=1.3$
$R_1=1$	2.464	2.707	2.988	3.404
$R_1=2$	3.399	3.925	4.523	5.398

Table I gives the sonic point R_* corresponding to four different values of Q_0 when $E_0 = -0.8755$. From Eq. (2.7) it can be seen that the negative value term E_0/Q_0 in the singular numerator decreases as Q_0 increases, so that the critical radius R_* is small if more heat is supplied. For moderate values of R, the positive term in the singular numerator decreases with the increase of R_1, so that R_* increases with the progress of the region of heat supply. The critical radius is approximately three solar radii.

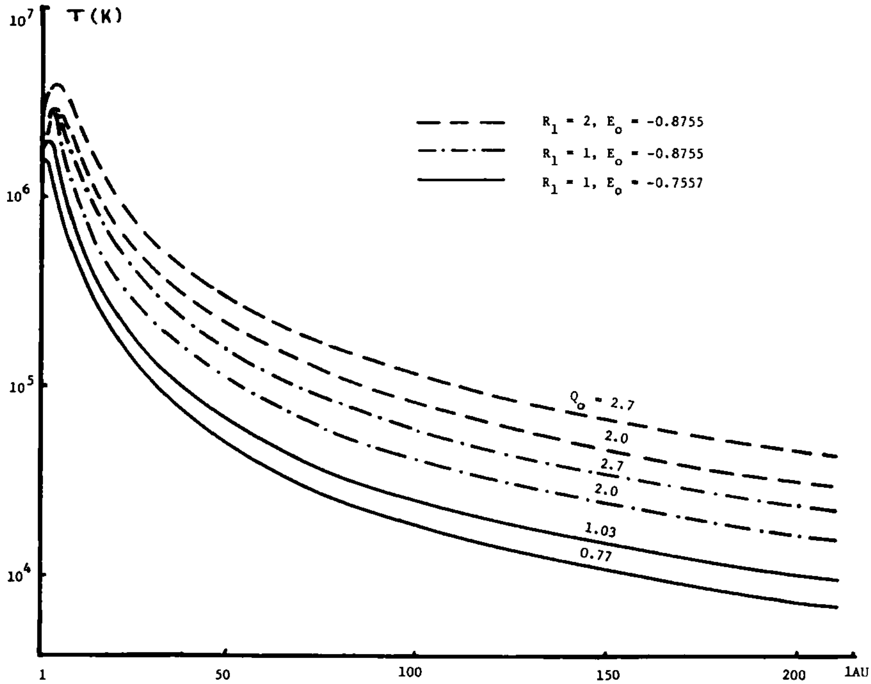

FIGURE 7 Several typical temperature distributions of the soldar wind.

The specific calculations given in this part indicate the influence of the heating of the solar wind parameters. There is obviously considerable fortuity in the distribution of the energy source in (3.1). But these results given the accelerating mechanism and qualitative trends of both the high-speed stream from the coronal hole and the normal flow of the solar wind.

4. CONCLUSION

We have discussed the influence of the magnitude and distribution of the energy flux in the corona on the accelerating process of the solar wind. The results of both the qualitative analysis and the quantitative calculation show that the magnitude of the solar wind speed depends mainly on the magnitude of the energy supplied to the solar wind, and the influence of the initial temperature at the lower corona is secondary. The larger the extension of the heat energy, the higher the temperature of the solar wind at the destination. When $R_1 = 2$, the temperature near the earth's orbit may reach 5×10^4 K, which agrees with the value of observation.

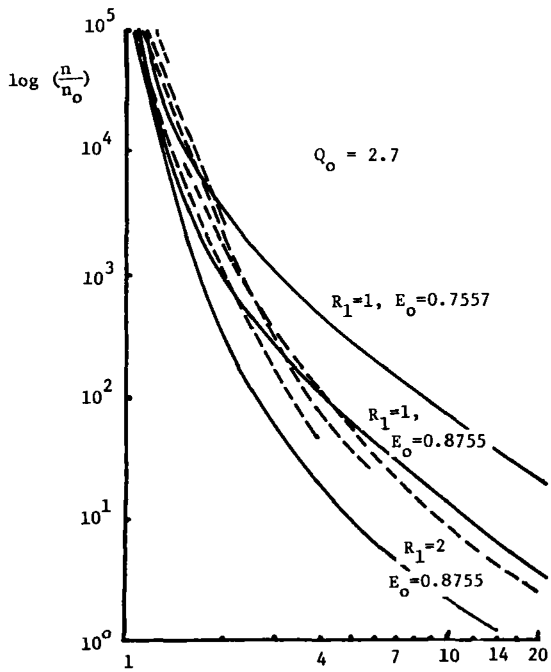

FIGURE 8 Plasma density profiles in the corona. The dotted lines show the results of observations, and the filled lines express the results of calculations.

The analysis of the singular points shows that there may be more than one sonic point. In the case of the heat energy being continuously supplied to the solar wind, there may be two sonic points, of which one must be a saddle point, making it possible for the solar wind to have smooth transonic flow. The position of the sonic point is near three solar radii.

Here, an explanation of the mechanism of the high-speed stream from the corona is suggested. The accelerating mechanism of the solar wind is generally common to all flows, but we obtain the high-speed stream for the coronal hole and the low velocity flow for the normal region of corona, according to the configuration and the heating process confined by the magnetic field in the corona. The difference between these two cases is graduated.

The satellite which will be launched in the near future to fly near the sun will be able to measure directly the parameters of the solar wind near ten solar radii. The results of these measurements will be very valuable in checking the various solar wind theories.

Acknowledgments

The author expresses his heartfelt thanks to S. T. Wu, L. Wang and M. L. Xue for helpful discussion, and many thanks are also due to T. E. Holzer, who informed the author of his interesting research in this subject.

References

Barnes, A., "Theoretical studies of the large-scale behavior of the solar wind," *Adv. Electronics & Electron Phys.* **36,** 1 (1974).

Cheng, C.-C., Doschek, G. A. and Feldman, U., "The dynamical properties of the solar corona from intensities and line widths of EUV forbidden lines of SiVIII, FeXI and FeXII," *Astrophys. J.* **227,** 1037 (1979).

Holzer, T. E., "Effects of rapidly diverging flow, heat addition and momentum addition in the solar wind and stellar winds," *J. Geophys. Res.* **82,** 23 (1977).

Hu, W. R., Ch. 9 in *The Solar Flare* (W. R. Hu *et al.*, eds.), Publ. of Chinese Academy of Sciences (1982). (In Chinese.)

Kopp, R. A. and Holzer, T. E., "Dynamics of coronal hole regions," *Sol. Phys.* **49,** 43 (1976).

Leer, E. and Holzer, T. E., "Energy addition in the solar wind," *J. Geophys. Res.* **85A,** 4681 (1980).

Parker, E. N., "Dynamics of interplanetary gas and magnetic fields," *Astrophys. J.* **128,** 664 (1958).

Parker, E. N., *Interplanetary Dynamic Processes*, Interscience, New York (1965).

Rosner, R. and Vaiana, G. S., "Hydrostatic and dynamic models of solar coronal holes," *Astrophys. J.* **216,** 141 (1977).

Scarf, F. L., "The origin of the solar wind," *The Solar Wind* (R. J. Mackin and M. Neugebauer, eds.), p. 199, Pergamon Press (1966).

Whang, Y. C. and Chien, T. H., "Expansion of the solar wind in high-speed streams," *Astrophys. J.* **221,** 350 (1978).

Wentzel, D. G., "Coronal heating by Alfvén waves," *Sol. Phys.* **39,** 129 (1974).